AMERICAN SOCIETY FOR MICROBIOLOGY | mBio®

RESEARCH ARTICLE
Molecular Biology and Physiology

The Lipid A 1-Phosphatase, LpxE, Functionally Connects Multiple Layers of Bacterial Envelope Biogenesis

Jinshi Zhao,[a] Jinsu An,[b,c] Dohyeon Hwang,[b,c] Qinglin Wu,[a] Su Wang,[a] Robert A. Gillespie,[a] Eun Gyeong Yang,[b] Ziqiang Guan,[a] Pei Zhou,[a] Hak Suk Chung[b,c]

[a]Department of Biochemistry, Duke University Medical Center, Durham, North Carolina, USA
[b]Center for Theragnosis, Biomedical Research Institute, Korea Institute of Science and Technology, Seoul, Republic of Korea
[c]Division of Bio-Medical Science & Technology, KIST School, Korea University of Science and Technology, Seoul, Republic of Korea

ABSTRACT Although distinct lipid phosphatases are thought to be required for processing lipid A (component of the outer leaflet of the outer membrane), glycerophospholipid (component of the inner membrane and the inner leaflet of the outer membrane), and undecaprenyl pyrophosphate (C_{55}-PP; precursors of peptidoglycan and O antigens of lipopolysaccharide) in Gram-negative bacteria, we report that the lipid A 1-phosphatases, LpxEs, functionally connect multiple layers of cell envelope biogenesis in Gram-negative bacteria. We found that *Aquifex aeolicus* LpxE structurally resembles YodM in *Bacillus subtilis*, a phosphatase for phosphatidylglycerol phosphate (PGP) with a weak *in vitro* activity on C_{55}-PP, and rescues *Escherichia coli* deficient in PGP and C_{55}-PP phosphatase activities; deletion of *lpxE* in *Francisella novicida* reduces the MIC value of bacitracin, indicating a significant contribution of LpxE to the native bacterial C_{55}-PP phosphatase activity. Suppression of plasmid-borne *lpxE* in *F. novicida* deficient in chromosomally encoded C_{55}-PP phosphatase activities results in cell enlargement, loss of O-antigen repeats of lipopolysaccharide, and ultimately cell death. These discoveries implicate LpxE as the first example of a multifunctional regulatory enzyme that orchestrates lipid A modification, O-antigen production, and peptidoglycan biogenesis to remodel multiple layers of the Gram-negative bacterial envelope.

IMPORTANCE Dephosphorylation of the lipid A 1-phosphate by LpxE in Gram-negative bacteria plays important roles in antibiotic resistance, bacterial virulence, and modulation of the host immune system. Our results demonstrate that in addition to removing the 1-phosphate from lipid A, LpxEs also dephosphorylate undecaprenyl pyrophosphate, an important metabolite for the synthesis of the essential envelope components, peptidoglycan and O-antigen. Therefore, LpxEs participate in multiple layers of biogenesis of the Gram-negative bacterial envelope and increase antibiotic resistance. This discovery marks an important step toward understanding the regulation and biogenesis of the Gram-negative bacterial envelope.

KEYWORDS bacterial cell envelope biogenesis, lipid A 1-phosphate phosphatase, phosphatidylglycerol phosphate phosphatase, type 2 phosphatidic acid phosphatase (PAP2) superfamily, undecaprenyl pyrophosphate phosphatase

The Gram-negative bacterial cell envelope consists of three essential molecular architectures—the inner membrane, the peptidoglycan layer, and the outer membrane—that together protect bacteria against mechanical stress, maintain cell shape, and shield these microorganisms from the damage of detergents and antibiotics. These architectures are formed by distinct molecules, with phospholipids constituting the inner membrane and inner leaflet of the outer membrane, peptide-conjugated carbohydrates constituting the peptidoglycan layer, and lipopolysaccharides (LPS) anchoring

Citation Zhao J, An J, Hwang D, Wu Q, Wang S, Gillespie RA, Yang EG, Guan Z, Zhou P, Chung HS. 2019. The lipid A 1-phosphatase, LpxE, functionally connects multiple layers of bacterial envelope biogenesis. mBio 10:e00886-19. https://doi.org/10.1128/mBio.00886-19.

Invited Editor M. Stephen Trent, University of Georgia

Editor Nina R. Salama, Fred Hutchinson Cancer Research Center

Copyright © 2019 Zhao et al. This is an open-access article distributed under the terms of the Creative Commons Attribution 4.0 International license.

Address correspondence to Pei Zhou, peizhou@biochem.duke.edu, or Hak Suk Chung, hschung@kist.re.kr.

J.Z., J.A., D.H., and Q.W. contributed equally to this article.

Received 9 April 2019
Accepted 15 May 2019
Published 18 June 2019

Downloaded from http://mbio.asm.org/ on March 4, 2020 at DUKE UNIV

at the outer leaflet of the outer membrane through the hydrophobic lipid A moiety. As peptidoglycan, phospholipids, and LPS are synthesized through distinct pathways, how Gram-negative bacteria orchestrate the biogenesis and remodeling across three layers of the cell envelope for optimal bacterial growth and virulence remains incompletely understood.

As the major lipid species coating the outer surface of Gram-negative bacteria, lipid A is the predominant signaling molecule that is detected by the mammalian Toll-like receptor 4 (TLR4)/myeloid differentiation factor 2 (MD-2) innate immune receptor (1) and caspase-4/-5/-11 (2) to trigger the host innate immune response to bacterial infection. With few exceptions, Gram-negative bacteria constitutively synthesize the 1,4′-bisphosphorylated tetra-acyl-lipid A intermediate, 3-deoxy-D-manno-oct-2-ulosonic acid (Kdo)-linked lipid IV_A (Kdo_2-lipid IV_A), via the action of seven conserved enzymes in the Raetz pathway (3) (see Fig. S1A in the supplemental material), which are essential to nearly all Gram-negative bacteria and are attractive targets for novel antibiotics (4–6). Gram-negative bacteria additionally harbor modification enzymes that further process the Kdo_2-lipid IV_A intermediate to generate unique lipid A molecules in each bacterial species to adapt to environmental changes and evade the host immune response (7). For example, the lipid A 1-phosphate is a key determinant for lipid A recognition by the mammalian TLR4/MD-2 innate immune receptor (8). Removal of the lipid A 1-phosphate by the membrane-embedded phosphatase LpxE strongly protects bacteria against host cationic peptides and the last-resort antibiotic colistin (9), significantly dampens the host innate immune response, and dramatically increases colonization and survival of *Helicobacter pylori* in the gastric mucosa (10).

In order to gain molecular insights into the structure and function of the lipid A 1-phosphatase LpxE, we identified the previously uncharacterized gene *aq_1706* from *Aquifex aeolicus* as the gene for the thermophilic LpxE enzyme ($LpxE_{AA}$). Our structural analysis of $LpxE_{AA}$ shows distinct features between $LpxE_{AA}$ and *Escherichia coli* PgpB ($PgpB_{EC}$) enzymes but reveals a surprising structural similarity to YodM, a phosphatase of phosphatidylglycerol phosphate (PGP) in the Gram-positive bacterium *Bacillus subtilis* with a weak *in vitro* activity on undecaprenyl pyrophosphate (C_{55}-PP). Consistent with our structural analysis, we found that $LpxE_{AA}$ possesses substantial *in vitro* activities toward Kdo_2-lipid A/lipid IV_A, C_{55}-PP, and PGP and complements *E. coli* strains deficient in C_{55}-PP phosphatase and PGP phosphatase activities. In addition to the LpxE enzyme from *A. aeolicus*, distant LpxE orthologs from *Francisella*, *Helicobacter*, and *Rhizobium* also complement *E. coli* strains deficient in the C_{55}-PP phosphatase activity, supporting the notion that the multifunctional lipid phosphatase activity is a general feature of LpxE enzymes. Significantly, deletion of the native *lpxE* gene sensitizes *Francisella novicida* to bacitracin, an antibiotic that sequesters C_{55}-PP to disrupt peptidoglycan synthesis; furthermore, suppression of plasmid-encoded *lpxE* in the *F. novicida* strain deficient in the endogenous C_{55}-PP phosphatase activity results in noticeable changes in cell morphology, profound reduction of O-antigen repeats in LPS, and loss of cell viability. Taken together, these observations reveal a previously unappreciated contribution of LpxE to peptidoglycan biogenesis and LPS O-antigen modification beyond its well-recognized role as the lipid A 1-phosphatase to orchestrate the remodeling of multiple layers of the Gram-negative bacterial envelope to respond to environmental changes, evade host immune surveillance, and promote bacterial viability and virulence.

RESULTS

A distant ortholog of $LpxE_{FN}$ in *A. aeolicus*. LpxE is a member of the lipid phosphatase/phosphotransferase (LPT) family, a well-distributed family of lipid-processing enzymes also known as the integral transmembrane branch of the type II phosphatidic acid phosphatase (PAP2) superfamily (11, 12). This family is characterized by a conserved tripartite active site motif of KX_6RP---PSGH---SRX_5HX_3D and activity independent of Mg^{2+} or other cations (13). The LPT family includes enzymes responsible for processing several types of lipids in Gram-negative bacteria, including the

Downloaded from http://mbio.asm.org/ on March 4, 2020 at DUKE UNIV

membrane-embedded PgpB, which dephosphorylates PGP and C_{55}-PP (14) (Fig. S2). Even though PgpB and LpxE are both members of the LPT family, they have been reported to have distinct substrate specificities: PgpB is unable to utilize lipid A as a substrate (15), whereas purified LpxE from *Rhizobium leguminosarum* ($LpxE_{RL}$) utilizes PGP ~1,000 times less efficiently than lipid A species as a substrate *in vitro* (16).

In order to gain a molecular understanding of the LpxE structure and function, we searched for a thermophilic LpxE enzyme from *Aquificae* to facilitate structural analysis. The lipid A of *Aquifex pyrophilus* LPS contains D-galacturonic acid in place of phosphates at the 1- and 4′-positions (17) (Fig. S1B). As the 1,4′-bisphosphorylated lipid IV_A is a common lipid A intermediate before further modification (18, 19) and as *Aquificae* has the conserved biosynthetic enzymes to make 1,4′-bisphosphorylated lipid IV_A, incorporation of the D-galacturonic acid moiety requires the removal of 1-phosphate from lipid A, indicating the presence of the lipid A 1-phosphatase activity in *Aquificae*. Such a rationale led us to search for the gene responsible for the lipid A 1-phosphatase activity in *A. aeolicus* VF5, as no lipid A 1-phosphatase has been reported in any *Aquifex* species.

A Position-Specific Iterated Basic Local Alignment Search Tool (PSI-BLAST) (20) search revealed a distant ortholog of *F. novicida* LpxE ($LpxE_{FN}$) (15), Aq_1706 (E value, 0.81; sequence identity, 13.84%), in the genome of *A. aeolicus* VF5. Aq_1706 shares little sequence identity with other LpxE enzymes (sequence identities of Aq_1706 with LpxE of *Helicobacter* and *Rhizobium* are 16.58% and 14.57%, respectively), except for the well-conserved tripartite active-site motif of KX_6RP---PSGH---SRX_5HX_3D (Fig. S3). In order to determine if *aq_1706* encodes the lipid A 1-phosphatase activity *in vivo*, we overexpressed Aq_1706 in the heptose transferase-deficient *E. coli* strain WBB06, which produces Kdo_2-lipid A instead of full-length LPS, to facilitate mass spectrometry analysis of lipid A modifications (21). Since *E. coli* does not encode LpxE activity, mass spectrometry analysis of the extracted lipids showed normal lipid A containing 1-phosphate with an *m/z* of 1,117.633 for the $[M\text{-}2H]^{2-}$ ion species (calculated *m/z*, 1,117.661 for the exact mass of 2,237.336 of Kdo_2-lipid A) from *E. coli* cells expressing a control vector; in contrast, overexpression of Aq_1706 in *E. coli* led to the disappearance of the intact lipid A species and significant accumulation of lipid A molecules lacking the 1-phosphate group, with an *m/z* of 1,077.647 for the $[M\text{-}2H]^{2-}$ ion species (calculated *m/z*, 1,077.678 for the exact mass of 2,157.370 of 1-dephospho Kdo_2-lipid A), consistent with the anticipated lipid A 1-phosphatase activity (Fig. 1A). In order to verify that the loss of phosphate occurred at the 1-position, but not at the 4′-position, we further tested the ability of LpxE to dephosphorylate 4′-^{32}P-labeled Kdo_2-lipid IV_A, which was previously shown to be an efficient substrate for LpxE enzymes with specific activity comparable to that for the substrate Kdo_2-lipid A (16). We found that treatment of Kdo_2-[4′-^{32}P] lipid IV_A with membrane extracts from *E. coli* overexpressing Aq_1706, but not those carrying a control vector, resulted in time-dependent reduction of the Kdo_2-lipid IV_A band and accumulation of an upper-shifted band on the thin-layer chromatography (TLC) plate (Fig. 1B), reflecting the removal of 1-phosphate but retention of the ^{32}P-labeled 4′-phosphate group. Taken together, these observations verify *aq_1706* in *A. aeolicus* as the gene that encodes the thermophilic lipid A 1-phosphatase LpxE ($LpxE_{AA}$).

Structural analysis of $LpxE_{AA}$ reveals a striking similarity to YodM in *B. subtilis*. After verifying the lipid A 1-phosphatase activity of $LpxE_{AA}$, we cloned and purified $LpxE_{AA}$. Consistent with the TMHMM analysis (http://www.cbs.dtu.dk/services/TMHMM/), high-yield expression of $LpxE_{AA}$ was achieved in a maltose-binding protein (MBP) fusion construct containing an N-terminal PelB secretion signal (22), suggesting that the N terminus of $LpxE_{AA}$ is located at the periplasmic side of the inner membrane. The crystal structure of $LpxE_{AA}$ containing an I63M mutation was determined at 2.38 Å (Fig. 2A; statistics shown in Table S1). The selenomethionine substitution of the nonconserved I63 residue (I63M) was designed to enhance the selenium single anomalous dispersion (Se-SAD) signal for *de novo* phasing. The overall structure of $LpxE_{AA}$ contains seven α-helices, including an N-terminal amphiphilic helix lying at

Downloaded from http://mbio.asm.org/ on March 4, 2020 at DUKE UNIV

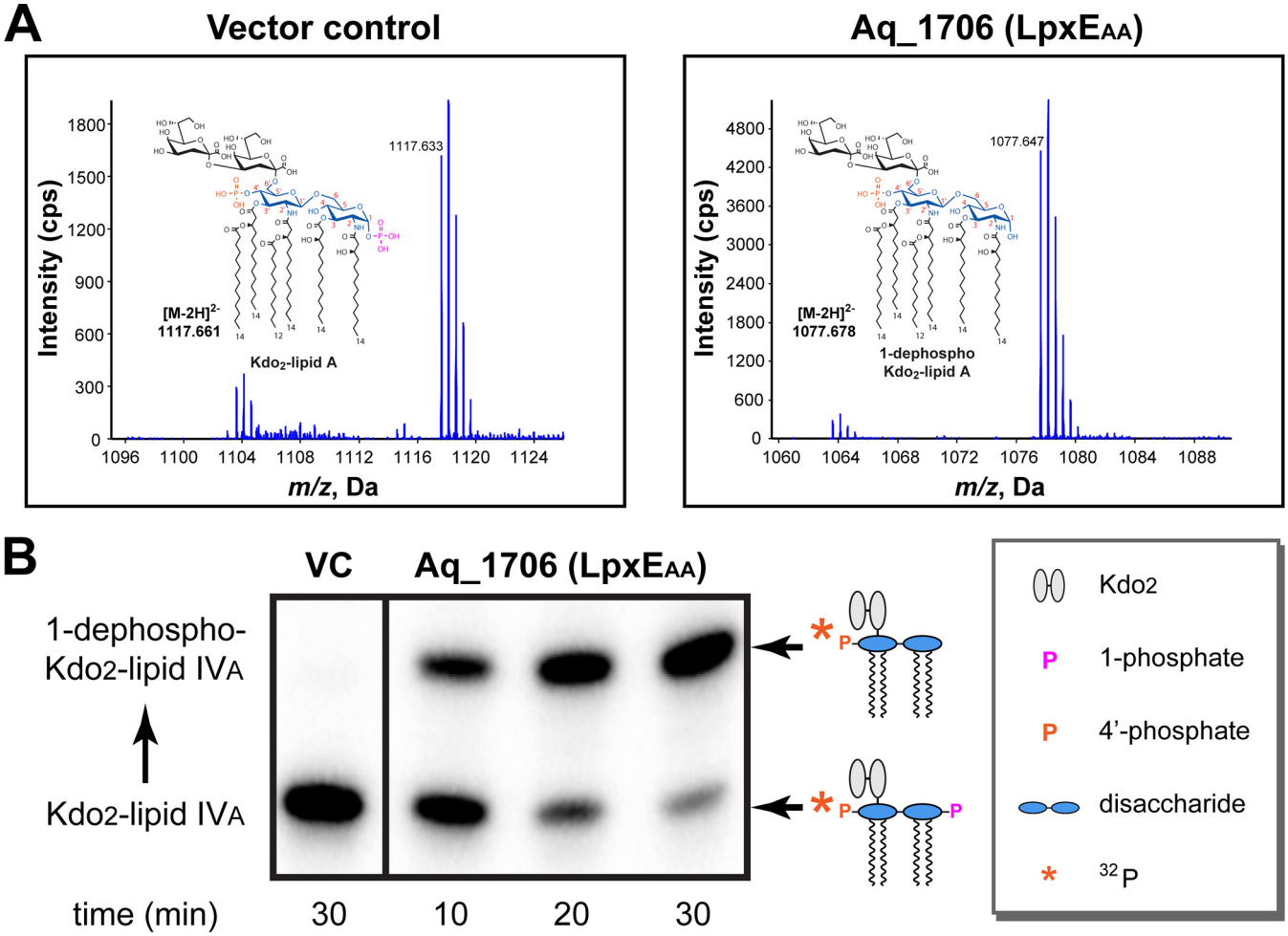

FIG 1 Characterization of Aq_1706 from *A. aeolicus* as the lipid A 1-phosphatase $LpxE_{AA}$. (A) Mass spectrometry analysis of lipid A species in the heptose-deficient *E. coli* strain WBB06 (left) and the WBB06 strain overexpressing $LpxE_{AA}$ (right). (B) ^{32}P-autoradiographic TLC-based Kdo_2-lipid IV_A 1-dephosphorylation assay of the membrane extract of the C41(DE3) strain overexpressing $LpxE_{AA}$.

the periplasmic surface of the inner membrane and five tightly packed transmembrane helices (α3 to α7). Apart from α2, which originates from the periplasmic surface and penetrates halfway across the inner membrane at an ~45° angle and immediately connects to transmembrane helix α3, the remaining helices are oriented largely in parallel or antiparallel with each other and perpendicularly to the membrane plane. Looking from the periplasmic surface, helix 5 (α5) is located at the center, which is surrounded by α2, α3, α4, α7, and α6 in a counterclockwise fashion (Fig. 2B).

The active site of LpxE is located at the periplasmic surface of the inner membrane and is defined by conserved motifs specific to the PAP2 enzymes ($\underline{K}^{73}X_6\underline{R}^{80}P$---$\underline{R}^{137}X_5\underline{H}^{143}X_3\underline{D}^{147}$) located at the C-terminal end of α4, the α4-α5 loop, α6, the α6-α7 loop, and the N terminus of α7 (Fig. 2C). Fortuitously, a sulfate molecule is found in the active site, which is a structural analog of the 1-phosphate group of lipid A. The sulfate group is extensively recognized by K73 and R80 of the $K^{73}X_6R^{80}P$ motif and R137 of the $R^{137}X_5H^{143}X_3D^{147}$ motif. The catalytically important H143 is located 3.3 Å away from the sulfur atom of the sulfate group, ready to carry out inline attack to remove the phosphate group of the lipid substrate. D147, the last residue of the $R^{137}X_5H^{143}X_3D^{147}$ motif, forms a hydrogen bond with H143. Although the corresponding aspartate residue is found in most LpxE enzymes (Fig. S3), it is absent in the LpxE ortholog from *H. pylori* ($LpxE_{HP}$), suggesting that it is not absolutely required for catalysis. The first three residues of the PSGH motif are conserved in $LpxE_{AA}$, with the central serine

Downloaded from http://mbio.asm.org/ on March 4, 2020 at DUKE UNIV

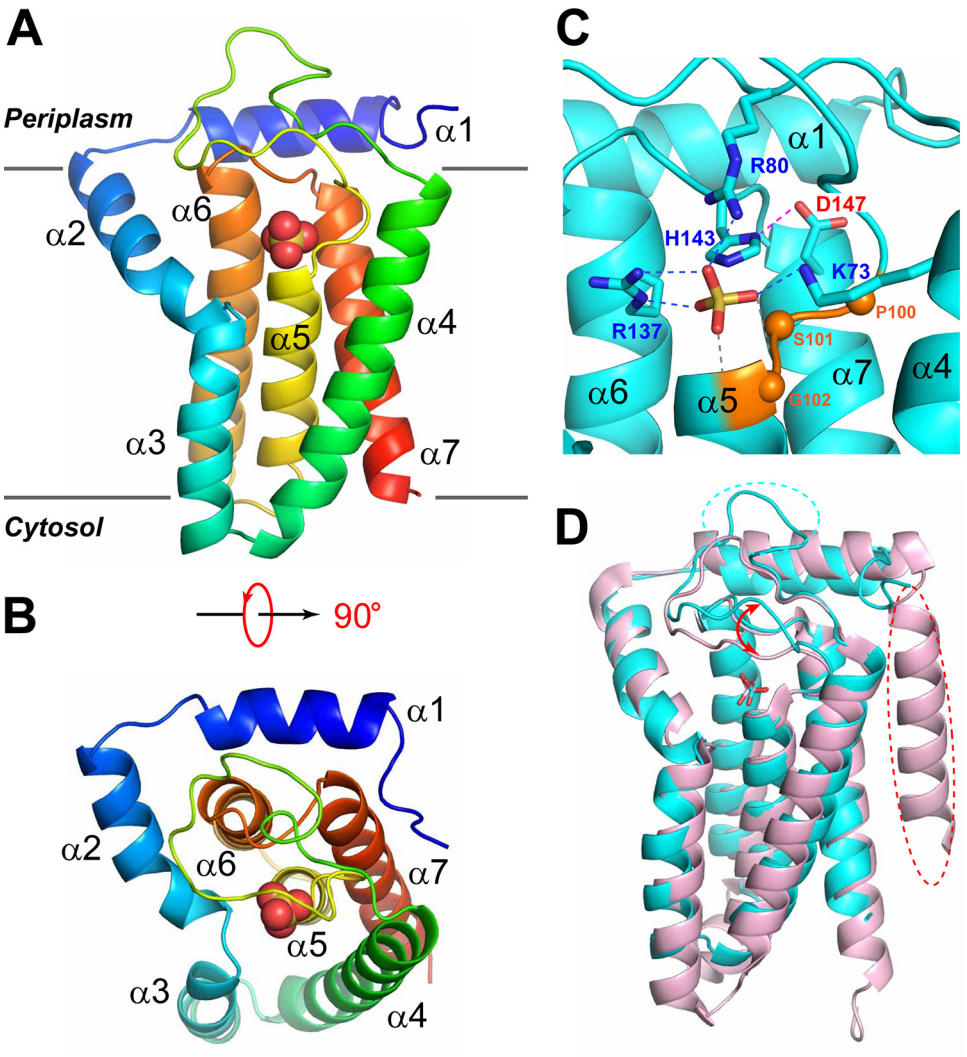

FIG 2 Crystal structure of $LpxE_{AA}$. (A) Ribbon representation of $LpxE_{AA}$, with blue to red colors corresponding to the N to C termini. The sulfate molecule is shown in the space-filling model. Individual helices and membrane locations are labeled. (B) Top view of $LpxE_{AA}$. (C) The active site of $LpxE_{AA}$. The sulfate molecule is shown in the stick model. Side chains of H143 and D147 from the RX_5HX_3D motif and conserved residues coordinating the sulfate molecule, including K73 and R80 from the KX_6RP motif and R137 of the RX_5HX_3D motif, are shown in the stick model. Hydrogen bonds are shown by dashed lines. The sulfate group is additionally stabilized by the interaction with the electrical dipole of helix $\alpha5$ (indicated by gray hydrogen bonds). The conserved PSG motif is colored in coral, with Cα atoms shown in spheres. (D) Superimposition of $LpxE_{AA}$ (cyan) with $YodM_{BS}$ (PDB code 5JKI; pink), revealing striking structural similarities. The major differences between the two structures are highlighted, with dashed circles indicating missing structural features (helix or loop) and arrows indicating conformational discrepancy.

residue (S101) serving as a helix cap to stabilize helix $\alpha5$, but the histidine residue is replaced with an aspartate residue in $LpxE_{AA}$ (Fig. 2C).

The $LpxE_{AA}$ structure shows noticeable conformational discrepancy with the previously reported structures of $PgpB_{EC}$ (PDB codes 4PX7 and 5JWY) (23, 24), another PAP2 family enzyme, with overall backbone root mean square deviations (RMSDs) of ~4.5 Å (Fig. S4); surprisingly, $LpxE_{AA}$ is structurally similar to the recently reported YodM in *B. subtilis* (PDB code 5JKI) (25), a PGP phosphatase with a weak *in vitro* activity on C_{55}-PP, with an overall backbone RMSD of 1.2 Å (Fig. 2D). The major differences of these two enzymes are the absence of an N-terminal transmembrane helix in $LpxE_{AA}$ in comparison with YodM, a longer $\alpha4$-$\alpha5$ loop in $LpxE_{AA}$, and a significant conformational variation of the $\alpha4$-$\alpha5$ loop surrounding the active site.

$LpxE_{AA}$ is a trifunctional lipid phosphatase *in vitro* and functionally complements *E. coli* mutants deficient in C_{55}-PP or PGP phosphatase activities. Surprised

Downloaded from http://mbio.asm.org/ on March 4, 2020 at DUKE UNIV

TABLE 1 Specific activities of enzymes in this study

Enzyme	Specific activity (μmol/mg/min)		
	Kdo_2-lipid A	C_{55}-PP	PGP
$LpxE_{AA}$	2.04 ± 0.46	3.58 ± 0.47	0.75 ± 0.11
$LpxE_{FN}$	3.25 ± 0.21	2.99 ± 0.45	0.038 ± 0.009
$UppP_{FN}$	0.010 ± 0.005	22.71 ± 2.62	0.031 ± 0.007

by the structural similarity between $LpxE_{AA}$ and $YodM_{BS}$, we asked whether $LpxE_{AA}$ could function as a C_{55}-PP and PGP phosphatase. To address this question, we compared the specific activities of purified $LpxE_{AA}$ toward Kdo_2-lipid A, PGP, and C_{55}-PP using the malachite green assay to detect the release of inorganic phosphate. As expected, $LpxE_{AA}$ efficiently catalyzed the hydrolysis of 1-phosphate from Kdo_2-lipid A, with a specific activity of 2.04 ± 0.46 μmol/mg/min. Moreover, $LpxE_{AA}$ catalyzed C_{55}-PP more efficiently than it catalyzed Kdo_2-lipid A, with a specific activity of 3.58 ± 0.47 μmol/mg/min—a value that is ~1.8-fold higher than that toward Kdo_2-lipid A. Finally, $LpxE_{AA}$ also displayed significant activity toward PGP, with a specific activity of 0.75 ± 0.11 μmol/mg/min, ~40% of its activity toward Kdo_2-lipid A (Table 1). Taken together, our biochemical assays validate $LpxE_{AA}$ as a trifunctional LPT enzyme that efficiently dephosphorylates chemically diverse Kdo_2-lipid A (glycolipids), PGP (phosphoglycerol lipid), and C_{55}-PP (isoprenyl lipid) *in vitro*.

In order to obtain further evidence of the trifunctional role of $LpxE_{AA}$ in cells, we examined whether $LpxE_{AA}$ could functionally rescue lethal *E. coli* mutants lacking C_{55}-PP phosphatase or PGP phosphatase activities. *E. coli* contains four C_{55}-PP phosphatases, BacA, PgpB, YbjG, and LpxT. A deletion mutant, Δ*ybjG* Δ*bacA* Δ*pgpB*::*kan*, in *E. coli* is lethal unless rescued by a plasmid expressing BacA, PgpB, or YbjG (26). To examine if $LpxE_{AA}$ could function as a C_{55}-PP phosphatase in cells, we set up complementation of the lethal Δ*ybjG* Δ*pgpB* Δ*bacA*::*kan E. coli* mutant carrying $lpxE_{AA}$ on a low-copy-number, temperature-sensitive pMAK705 vector (pMAK-$lpxE_{AA}$). The *E. coli bacA* gene, encoding the C_{55}-PP phosphatase, was used as the positive control (pMAK-$bacA_{EC}$). We found that overexpression of $LpxE_{AA}$ and $BacA_{EC}$ from pMAK705-derived plasmids complemented the lethal phenotype of the Δ*ybjG* Δ*pgpB* Δ*bacA*::*kan* triple knockout in *E. coli* on an LB agar plate at 30°C; such a complementation effect was lost when cells were grown at 42°C, consistent with the loss of the temperature-sensitive pMAK705 plasmid encoding $LpxE_{AA}$ or $BacA_{EC}$ and confirming that $LpxE_{AA}$ functionally complements the loss of C_{55}-PP phosphatase activity in *E. coli* (Fig. 3A).

We similarly tested whether $LpxE_{AA}$ functionally complements the loss of PGP phosphatase activity in *E. coli*. *E. coli* has three PGP phosphatases, PgpA, PgpB, and PgpC (27). A Δ*pgpA* Δ*pgpB* Δ*pgpC*::*kan* triple-knockout mutant is lethal unless it is rescued by a plasmid harboring an active PGP phosphatase (27). Overexpression of $LpxE_{AA}$ or the positive control $PgpA_{EC}$ from the temperature-sensitive pMAK705 plasmid supported the growth of the Δ*pgpA* Δ*pgpB* Δ*pgpC*::*kan* triple-knockout mutant strains at 30°C but not at 42°C. In contrast, the control strain (W3110/pMAK705) grew well at both temperatures (Fig. 3B). These observations confirm that $LpxE_{AA}$ is a functional PGP phosphatase in *E. coli*.

While the pMAK705 vector-encoded $LpxE_{AA}$ complemented *E. coli* triple knockouts lacking C_{55}-PP phosphatase or PGP phosphatase activities, pMAK705 has a higher copy number (pSC101 origin, ~5 copies/cell) than that of the chromosome in *E. coli* (single copy/cell). In order to mitigate the concern that the observed genetic complementation was caused by multiple copies of the $lpxE_{AA}$ gene, we replaced the *pgpB* gene in the chromosome of *E. coli* (BW25113) Δ*ybjG* Δ*bacA* with a gene cassette (P_L-$lpxE_{AA}$-*FRT-kan-FRT*) containing $lpxE_{AA}$ and a kanamycin resistance gene under the control of the P_L promoter (28). The resulting *E. coli* strain (*E. coli* BW25113 Δ*ybjG* Δ*bacA* Δ*pgpB*::P_L-$lpxE_{AA}$-*FRT-kan-FRT*) grew on an LB agar plate, and the proper knockouts of *bacA*, *ybjG*, and *pgpB* were verified by PCR (Fig. 3C), confirming that the chromosomal copy of $lpxE_{AA}$ complemented the loss of C_{55}-PP phosphatase activity. Using a similar approach,

Downloaded from http://mbio.asm.org/ on March 4, 2020 at DUKE UNIV

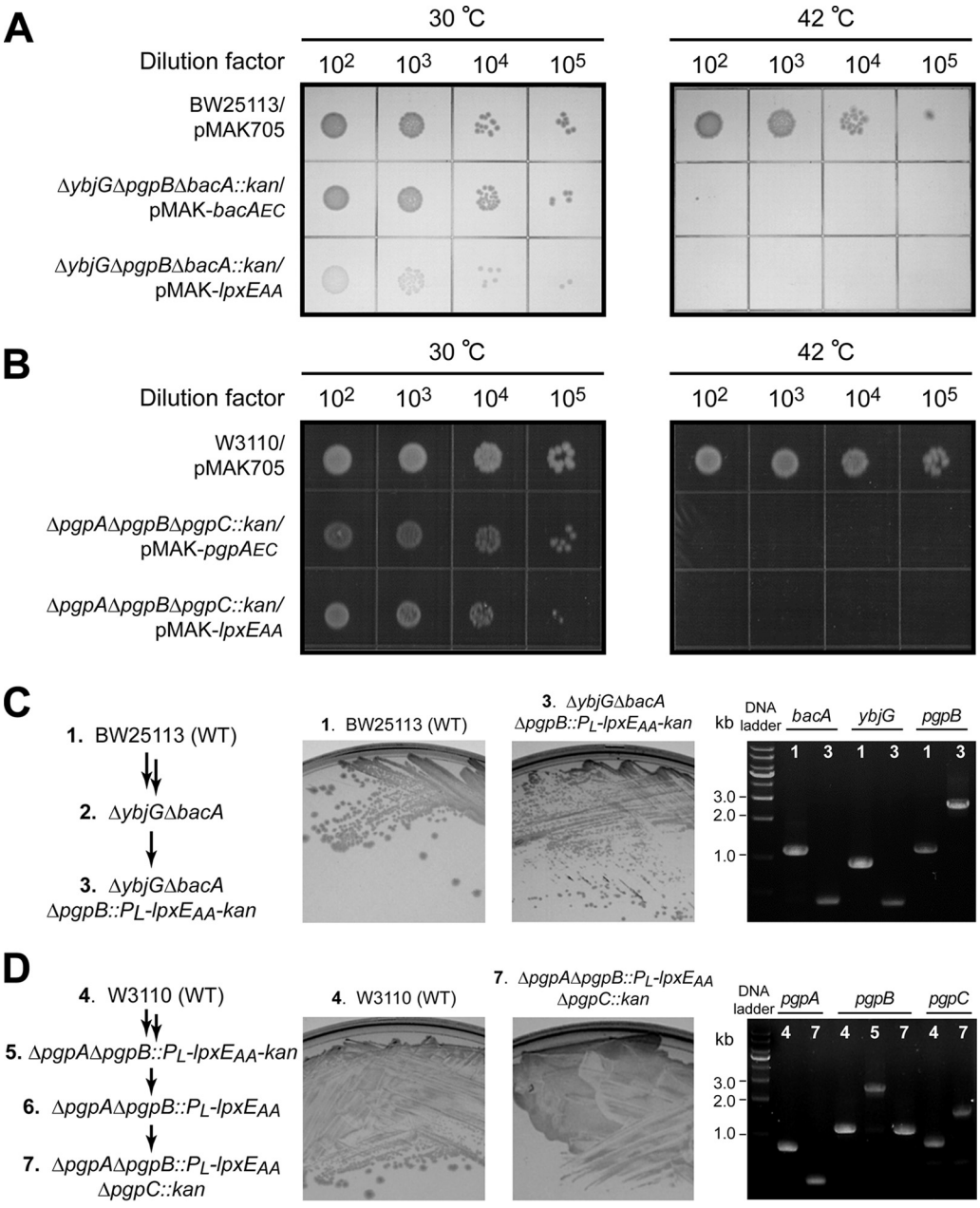

FIG 3 $LpxE_{AA}$ complements *E. coli* strains deficient in C_{55}-PP phosphatase or PGP phosphatase activities. (A) Complementation of the C_{55}-PP phosphatase-deficient *E. coli* strain (BW25113 Δ*ybjG* Δ*pgpB* Δ*bacA*::*kan*) by the temperature-sensitive pMAK705 plasmid harboring $bacA_{EC}$ (positive control, pMAK-$bacA_{EC}$) or $lpxE_{AA}$ (pMAK-$lpxE_{AA}$). WT *E. coli* cells carrying pMAK705 or C_{55}-PP phosphatase-deficient *E. coli* cells carrying pMAK-$bacA_{EC}$ or pMAK-$lpxE_{AA}$ were grown at 30°C or 42°C. From left to right are spots of 10-fold serial dilutions from 10^2 to 10^5. (B) Complementation of the PGP phosphatase-deficient *E. coli* strain (W3110 Δ*pgpA* Δ*pgpB* Δ*pgpC*::*kan*) by the temperature-sensitive pMAK705 plasmid harboring $pgpA_{EC}$ (positive control, pMAK-$pgpA_{EC}$) or $lpxE_{AA}$ (pMAK-$lpxE_{AA}$). WT *E. coli* cells carrying pMAK705 or PGP phosphatase-deficient *E. coli* cells carrying pMAK-$pgpA_{EC}$ or pMAK-$lpxE_{AA}$ were grown at 30°C or 42°C. From left to right are spots of 10-fold serial dilutions from 10^2 to 10^5. (C) Chromosomal complementation of C_{55}-PP phosphatase activity-deficient *E. coli* with $lpxE_{AA}$. The left, middle, and right images show the construction of different *E. coli* C_{55}-PP phosphatase gene deletion mutants, the growth of WT *E. coli* cells and C_{55}-PP phosphatase-deficient cells complemented by a chromosomal copy of $lpxE_{AA}$, and the PCR verification of *ybjG*, *bacA*, and *pgpB* knockouts of the target mutant strain, respectively. (D) Chromosomal complementation of PGP phosphatase activity-deficient *E. coli* with $lpxE_{AA}$. The left, middle, and right images show the construction of different *E. coli* PGP phosphatase gene deletion mutants, the growth of WT *E. coli* cells and PGP phosphatase-deficient cells complemented by a chromosomal copy of $lpxE_{AA}$, and PCR verification of *pgpA*, *pgpC*, and *pgpB* knockouts of the target mutant strain, respectively. Since the expected sizes of *pgpB* (1,106 bp) and *pgpB*::P_L-$lpxE_{AA}$ (1,093 bp) are similar using primers flanking *pgpB* in the final strain, the knockout of *pgpB* was established by also verifying the PCR result of the mother strain (strain 5: W3110 Δ*pgpA* Δ*pgpB*::P_L-$lpxE_{AA}$-*frt*-*kan*-*frt*).

Downloaded from http://mbio.asm.org/ on March 4, 2020 at DUKE UNIV

we also replaced the *pgpB* gene of *E. coli* (W3110) Δ*pgpA* with P_L-*lpxE*$_{AA}$-*FRT-kan-FRT*, removed the kanamycin resistance cassette (29), and then knocked out *pgpC*. The resulting strain (*E. coli* W3110 Δ*pgpA* Δ*pgpB*::P_L-*lpxE*$_{AA}$ Δ*pgpC*::*kan*) also grew on an LB agar plate, and knockouts of *pgpA*, *pgpB*, and *pgpC* were verified by PCR (Fig. 3D), confirming that the chromosomal copy of *lpxE*$_{AA}$ similarly complemented the loss of PGP phosphatase activity.

Altogether, the substantial phosphatase activities of LpxE$_{AA}$ toward Kdo$_2$-lipid A, C_{55}-PP, and PGP *in vitro* and its ability to complement the loss of C_{55}-PP and PGP phosphatase activities in *E. coli*—both via the plasmid-borne gene and via chromosomal knock-in—strongly support the multifunctionality of LpxE$_{AA}$ in Gram-negative bacterial envelope biogenesis.

LpxE$_{FN}$ is a bifunctional lipid phosphatase *in vitro* and functionally complements an *E. coli* mutant deficient in the C_{55}-PP phosphatase activity. Despite the intriguing observation of the multifunctionality of LpxE$_{AA}$, it is challenging to establish the biological consequence in its native host due to the difficulty of culturing and genetic manipulation of *A. aeolicus*. Therefore, we asked if other LpxE enzymes from genetically trackable bacteria similarly display multifunctional lipid phosphatase activities. In order to answer this question, we chose LpxE$_{FN}$, a distant ortholog of LpxE$_{AA}$, for further characterization. The ability of LpxE$_{FN}$ to dephosphorylate lipid A at the 1-position was previously reported (15), but its activity toward other lipid substrates has not been thoroughly investigated. We first conducted similar complementation experiments using *E. coli* strains deficient in either the C_{55}-PP phosphatase activity or PGP phosphatase activity carrying the temperature-sensitive pMAK-*lpxE*$_{FN}$. We found that LpxE$_{FN}$ complemented the loss of C_{55}-PP phosphatase activity of *E. coli* (Δ*ybjG* Δ*pgpB* Δ*bacA*::*kan*) at 30°C but not at 42°C, indicating that LpxE$_{FN}$ is a functional C_{55}-PP phosphatase in *E. coli* (Fig. 4A). However, we were unable to complement *E. coli* deficient in the PGP activity (Δ*pgpA* Δ*pgpB* Δ*pgpC*::*kan*) with a plasmid encoding LpxE$_{FN}$ (pMAK-*lpxE*$_{FN}$). Consistently, we found that purified LpxE$_{FN}$ displayed significant phosphatase activity toward both Kdo$_2$-lipid A and C_{55}-PP and processed these two substrates with similar efficiencies (specific activities of 3.25 ± 0.21 μmol/mg/min for Kdo$_2$-lipid A and 2.99 ± 0.45 μmol/mg/min for C_{55}-PP), but its activity toward PGP was ~100-fold lower (specific activity of 0.038 ± 0.009 μmol/mg/min) (Table 1), confirming that LpxE$_{FN}$ is a bifunctional lipid phosphatase.

***F. novicida* harbors two C_{55}-PP phosphatases: LpxE$_{FN}$ and FTN_1552.** It is important to note that the lipid A 1-phosphatase activity is not essential in bacteria but the C_{55}-PP phosphatase activity is. Prior to this study, no enzyme encoding the C_{55}-PP phosphatase activity had been identified in *F. novicida*. As the transposon mutant of *lpxE*$_{FN}$ is not lethal in *F. novicida* (30), we reasoned that there must exist another enzyme encoding the C_{55}-PP phosphatase activity in *F. novicida*. By searching for *F. novicida* proteins homologous to *E. coli* enzymes containing C_{55}-PP phosphatase activity (i.e., BacA$_{EC}$, YbjG$_{EC}$, PgpB$_{EC}$, and LpxT$_{EC}$) using PSI-BLAST (20), we have identified a PAP2 family protein of unknown function, FTN_1552, as a potential candidate of the C_{55}-PP phosphatase (PSI-BLAST of PgpB$_{EC}$: E value of 0.003 and sequence identity of 16.47%). We found that the temperature-sensitive pMAK705 vector harboring *ftn_1552* complemented the *E. coli* strain deficient in C_{55}-PP phosphatase activity (Δ*ybjG* Δ*pgpB* Δ*bacA*::*kan*), confirming *ftn_1552* as the gene encoding the C_{55}-PP phosphatase activity (Fig. 4A). FTN_1552 was subsequently renamed UppP$_{FN}$. Purified UppP$_{FN}$ appears to be a specific enzyme for C_{55}-PP, with a specific activity of 22.71 ± 2.62 μmol/mg/min, and displays little activity toward Kdo$_2$-lipid A and PGP (specific activities of 0.010 ± 0.005 μmol/mg/min and 0.031 ± 0.007 μmol/mg/min, respectively [Table 1]). Importantly, while *F. novicida* strains containing a chromosomal deletion of either *lpxE*$_{FN}$ or *uppP*$_{FN}$ were viable, we were unable to generate *F. novicida* strains containing both deletions (Δ*lpxE*$_{FN}$ Δ*uppP*$_{FN}$) in the chromosome (Fig. 4B and C). However, *F. novicida* cells were viable in the Δ*uppP*$_{FN}$ background when *lpxE*$_{FN}$ was replaced with *lpxE*$_{AA}$ (Fig. 4B and C). Furthermore, when *F. novicida* was first transformed with a

Downloaded from http://mbio.asm.org/ on March 4, 2020 at DUKE UNIV

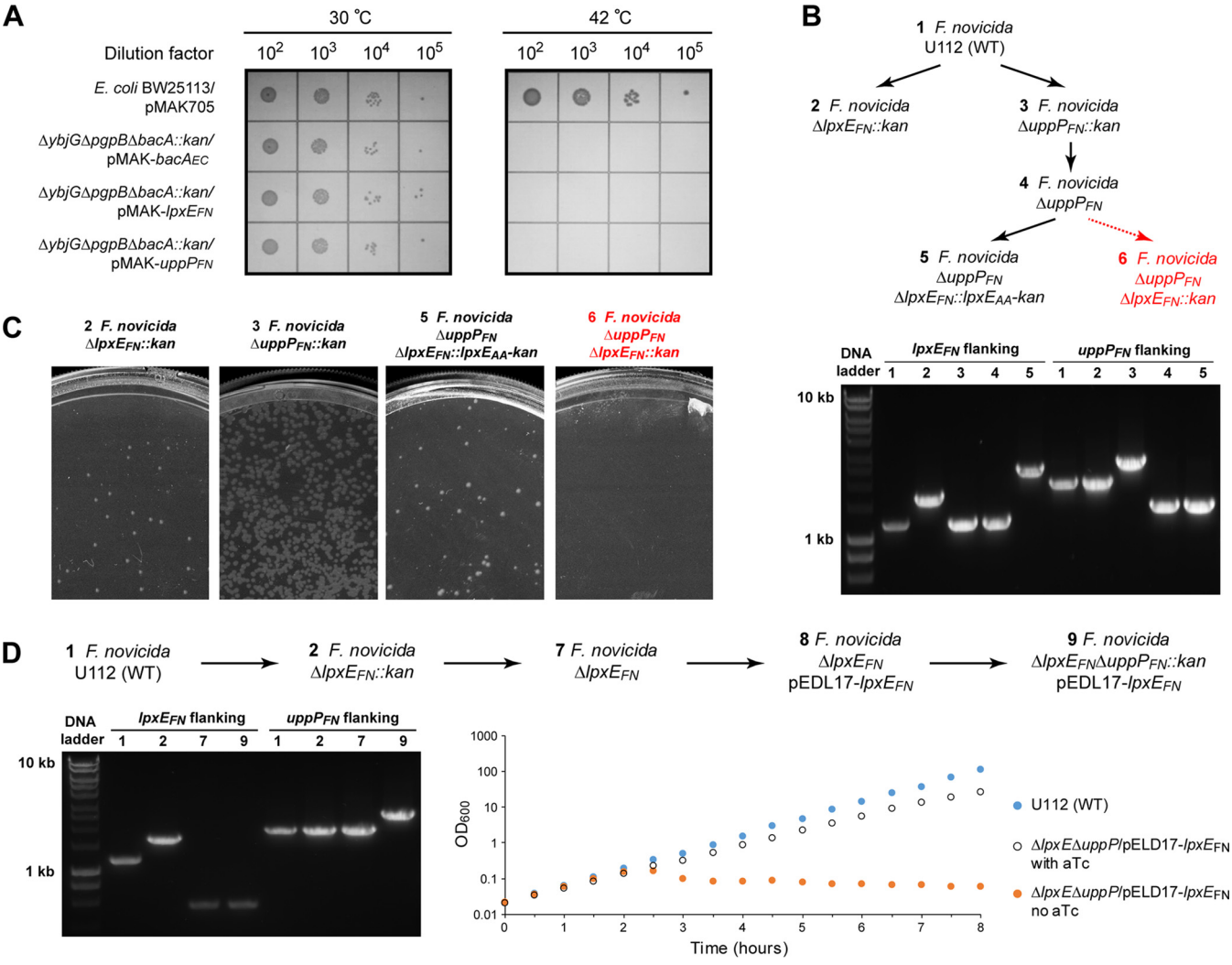

FIG 4 *F. novicida* harbors two C_{55}-PP phosphatases, $LpxE_{FN}$ and $UppP_{FN}$. (A) Complementation of the C_{55}-PP phosphatase-deficient *E. coli* strain (BW25113 Δ*ybjG* Δ*bacA* Δ*pgpB*::*kan*) by the temperature-sensitive pMAK705 plasmid harboring $bacA_{EC}$ (positive control, pMAK-$bacA_{EC}$), $lpxE_{FN}$ (pMAK-$lpxE_{FN}$), or $uppP_{FN}$ (*ftn_1552*, pMAK-$uppP_{FN}$). WT *E. coli* cells carrying pMAK705 or C_{55}-PP phosphatase-deficient *E. coli* cells carrying pMAK-$bacA_{EC}$, pMAK-$lpxE_{FN}$, or pMAK-$uppP_{FN}$ were grown at 30°C or 42°C. From left to right are spots of 10-fold serial dilutions from 10^2 to 10^5. (B) Schematic illustration of the construction of different *F. novicida* gene deletion strains. Viable and lethal strains are in black and red, respectively. The presence of the proper gene deletion was verified by PCR using primers at ~0.25-kb or 0.6-kb positions flanking *lpxE* or *uppP*, respectively. (C) Viability of *F. novicida* mutants. While *F. novicida* mutants containing Δ$lpxE_{FN}$::*kan*, Δ$uppP_{FN}$::*kan*, or Δ$uppP_{FN}$ Δ$lpxE_{FN}$::$lpxE_{AA}$ were viable, no colonies could be isolated for *F. novicida* mutants containing Δ$uppP_{FN}$ Δ$lpxE_{FN}$::*kan*. (D) Construction of the conditional lethal *F. novicida* strain containing Δ$lpxE_{FN}$ Δ$uppP_{FN}$ complemented by aTc-inducible pEDL17-$lpxE_{FN}$. The sequence of strain construction is shown at the top. The presence of the desired gene deletion was verified by PCR (left). Prolonged withdrawal of aTc from the growth medium resulted in a slow bactericidal phenotype (right).

plasmid (pEDL17) bearing $lpxE_{FN}$ under the control of an anhydrotetracycline (aTc) promoter, we were also able to obtain viable *F. novicida* colonies containing chromosomal deletions of both $lpxE_{FN}$ and $uppP_{FN}$ (U112 Δ$lpxE_{FN}$ Δ$uppP_{FN}$::*kan*/pEDL17-$lpxE_{FN}$). The presence of proper chromosomal deletions of the $lpxE_{FN}$ and $uppP_{FN}$ genes was verified by PCR (Fig. 4D). As expected, the viability of such a strain depends on the expression of plasmid-encoded $LpxE_{FN}$: prolonged withdrawal of aTc suppressed the bacterial growth and slowly resulted in cell lysis in culture (Fig. 4D), reinforcing the notion that $UppP_{FN}$ and $LpxE_{FN}$ share redundant C_{55}-PP phosphatase activities in *Francisella*.

$LpxE_{FN}$ functionally connects multiple layers of envelope biogenesis in *F. novicida*. After establishing that $LpxE_{FN}$ shares C_{55}-PP phosphatase activity with $UppP_{FN}$, we further examined the biological implication of the multifunctional enzymatic activity of $LpxE_{FN}$ in its native host, *F. novicida*. We first verified the role of $LpxE_{FN}$

Downloaded from http://mbio.asm.org/ on March 4, 2020 at DUKE UNIV

as a lipid A 1-phosphatase. Wild-type (WT) *F. novicida* cells contain both LPS (i.e., core oligosaccharide and O-antigen-modified Kdo-lipid A3 without 1- and 4′-phosphates) and free lipid A species A1 and A2, which do not contain core oligosaccharides/Kdo or O-antigen (lipid A2 differs from lipid A1 in that it has an additional α-linked glucose moiety attached to its 6′-position; also see the schematic lipid A structures of WT *F. novicida* in Fig. 5A) (31). Both lipid A1 and lipid A2 are further modified by FlmK, which transfers galactosamine from C_{55}-P-galactosamine to the 1-phosphate of lipid A (32, 33). As the core oligosaccharide and O-antigen-modified lipid A are inefficiently extracted by the Bligh-Dyer method for mass spectrometry analysis, we examined the effect of Δ*lpxE*$_{FN}$ in the *F. novicida* strain deficient in the glycosyltransferase activity (Δ*lpcC*), which produces Kdo-lipid A3 (instead of LPS), in addition to lipids A1 and A2 found in the wild-type cells (Fig. 5A). Accumulations of Kdo-(1-phospho)-lipid A3 and Kdo-(galactosamine-1-phospho)-lipid A3, as well as the disappearance of Kdo-lipid A3, were observed in *F. novicida* when *lpxE*$_{FN}$ was deleted (Δ*lpxE*$_{FN}$), confirming the lipid A 1-phosphatase activity of LpxE$_{FN}$ in cells (Fig. 5A and Fig. S5).

As the C_{55}-PP phosphatase activity of LpxE$_{FN}$ (2.99 $\pm$ 0.45 μmol/mg/min) is only ~7-fold smaller than that of UppP$_{FN}$ (22.71 $\pm$ 2.62 μmol/mg/min), we asked whether LpxE$_{FN}$ could functionally contribute to the bacterial envelope biogenesis beyond lipid A modification at the 1-phosphate position. We first compared the sensitivities of the wild-type *F. novicida* strain (U112) and mutant strains containing either the *lpxE* or *uppP* deletion to bacitracin, an antibiotic sequestering C_{55}-PP. We found that while the loss of *uppP* in *F. novicida* generated an 8.5-fold drop of MIC in comparison with that of the WT strain (0.5 μM versus 4.25 μM), as expected, the loss of *lpxE* also resulted in ~1.7-fold drop of the MIC of bacitracin (2.5 μM for *F. novicida* Δ*lpxE*) (Fig. 5B), implicating a functional role of LpxE$_{FN}$ in the recycling of C_{55}-PP.

In order to isolate the biological effect of LpxE$_{FN}$, we utilized the *F. novicida* strain containing chromosomal deletions of both *uppP*$_{FN}$ and *lpxE*$_{FN}$, which is complemented by a plasmid carrying *lpxE*$_{FN}$ under the control of an aTc promoter. We found that the loss of plasmid-mediated expression of LpxE$_{FN}$ due to withdrawal of aTc in the growth medium resulted in cell enlargement, reflecting defective peptidoglycan biosynthesis (Fig. 5C). Strikingly, while no change of O-antigen repeats was observed in *F. novicida* cells containing the chromosomal deletion of either *lpxE* or *uppP* in comparison with WT cells (Fig. 5D), transient suppression of LpxE led to a dramatic reduction of the LPS O-antigen repeats, including both high- and low-repeat species (Fig. 5E) (34), suggesting a contribution of LpxE to the O-antigen biogenesis. These observations are consistent with the notion that the biosynthesis and transport of peptidoglycan and O-antigen depend on C_{55}-P, the product of LpxE$_{FN}$ (and UppP$_{FN}$) activity, and reveal a previously unappreciated function of LpxE in the biogenesis and remodeling of multiple components across the bacterial envelope: peptidoglycan, free lipid A, and the O-antigen repeat of LPS.

DISCUSSION

LpxE enzymes are important virulence factors that promote bacterial survival, fitness, and pathogenicity. In *H. pylori* and *Rhizobium etli* CE3, the chromosomal knockout of *lpxE* resulted in increased susceptibility to positively charged antimicrobial peptides such as polymyxin B and colistin (9, 35), presumably due to the retention of 1-phosphate of lipid A. Previous studies showed that *Rhizobium* LpxE displays over a 1,000-fold preference of Kdo_2-lipid A/lipid IV_A over PGP; therefore, LpxE has been regarded as a highly specific monofunctional enzyme whose sole activity is to remove the 1-phosphate from lipid A. In this study, based on the striking structural similarity between LpxE$_{AA}$ and YodM$_{BS}$, a PGP phosphatase with a weak *in vitro* activity on C_{55}-PP phosphatase, we discovered that LpxE is a multifunctional lipid phosphatase. The LpxE enzyme from *A. aeolicus* displays significant activities toward Kdo_2-lipid A/lipid IV_A, C_{55}-PP and PGP and functionally complements *E. coli* strains deficient in C_{55}-PP or PGP phosphatase activities. Likewise, the LpxE enzyme from *F. novicida* is a dual-function enzyme that processes Kdo_2-lipid A and C_{55}-PP with similar efficiencies. Strikingly,

Downloaded from http://mbio.asm.org/ on March 4, 2020 at DUKE UNIV

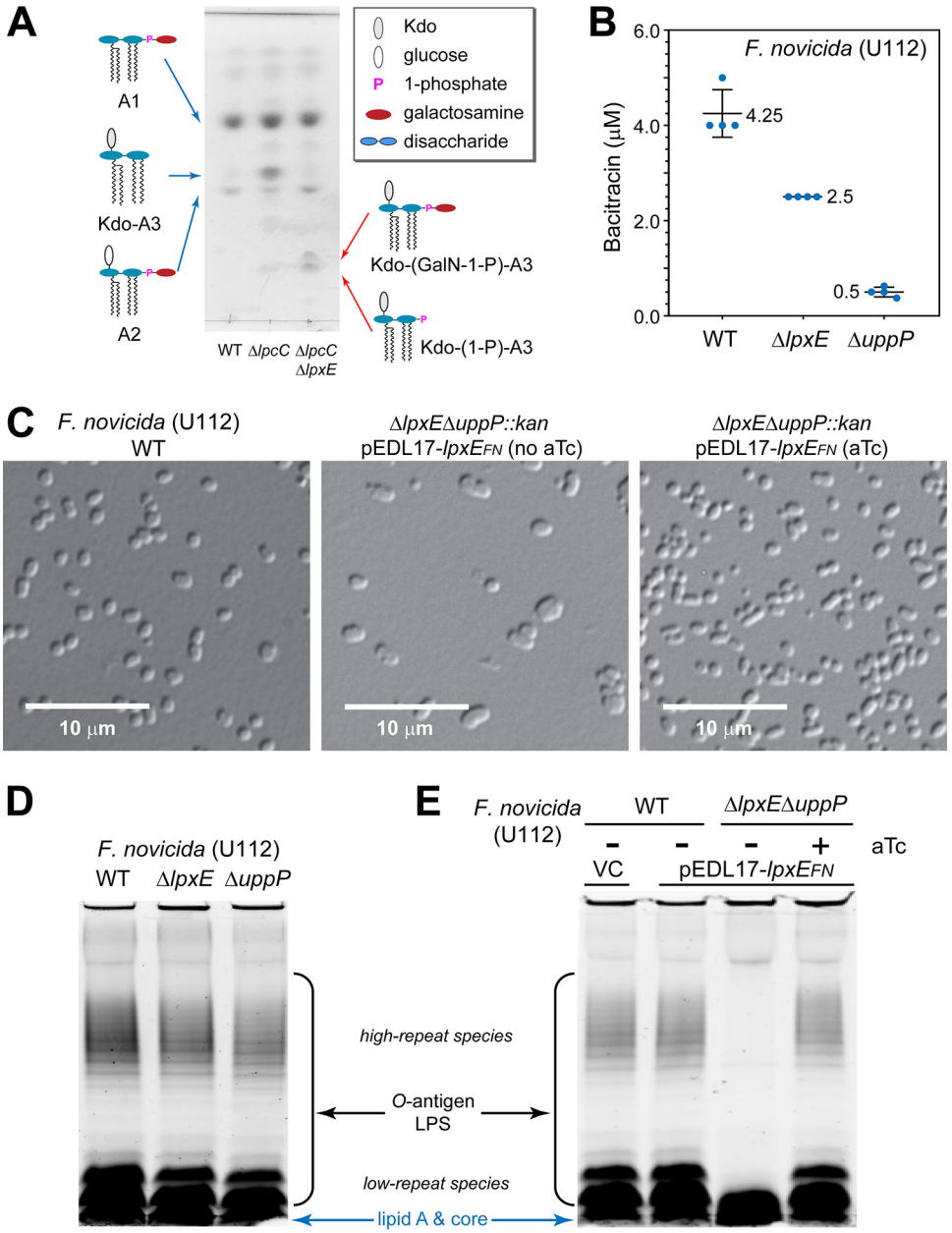

FIG 5 $LpxE_{FN}$ functionally contributes to multiple layers of the *F. novicida* bacterial envelope biogenesis. (A) Deletion of $lpxE_{FN}$ results in accumulation of 1-phosphorylated Kdo-lipid A3 species. The profiles of total lipid extracts from *F. novicida* U112 WT, Δ*lpcC*, and Δ*lpcC* Δ*lpxE* strains were analyzed by TLC. Lipid A species are labeled. Abbreviations: GalN, galactosamine; A1, lipid A1; A2, lipid A2; Kdo-A3, Kdo-lipid A3; Kdo-(galactosamine-1-phospho)-lipid A3; Kdo-(1-P)-A3, Kdo-(1-phospho)-lipid A3. (B) Deletion of $lpxE_{FN}$ sensitizes *F. novicida* to bacitracin as reflected by reduced MIC. Error bars represent standard deviations from quadruplet measurements. (C) Suppression of the plasmid-encoded $LpxE_{FN}$ expression in the Δ$lpxE_{FN}$ Δ$uppP_{FN}$::*kan* mutant of *F. novicida* causes cell deformation. Images of wild-type cells and Δ$lpxE_{FN}$ Δ$uppP_{FN}$::*kan F. novicida* mutant cells without and with $LpxE_{FN}$ expression are shown in the left, middle, and right images, respectively. (D) Lack of LPS phenotypes in *F. novicida* cells containing the single deletion of $lpxE_{FN}$ or $uppP_{FN}$. (E) Suppression of the plasmid-encoded $LpxE_{FN}$ expression in the Δ$lpxE_{FN}$ Δ$uppP_{FN}$::*kan* mutant of *F. novicida* causes the loss of O-antigen repeats in LPS. LPS profiles from wild-type *F. novicida* cells carrying the pDEL17 vector (VC) or the C_{55}-PP phosphatase-deficient (Δ$lpxE_{FN}$ Δ$uppP_{FN}$::*kan*) cells carrying the pDEL17-$lpxE_{FN}$ vector without or with aTc were analyzed on SDS-PAGE gels using the Pro-Q Emerald LPS staining kit. O-antigen-containing LPS, including both high- and low-repeat species, and free lipid A/core species are labeled.

deletion of $lpxE_{FN}$ in its native host *F. novicida* resulted in accumulation of phosphorylated lipid A species and increased sensitivity to bacitracin; in the C_{55}-PP phosphatase-deficient (Δ*uppP* and Δ*lpxE* double-knockout mutant) *F. novicida*, suppression of $LpxE_{FN}$ expression from the plasmid resulted in cell deformation due to defective peptidogly-

Downloaded from http://mbio.asm.org/ on March 4, 2020 at DUKE UNIV

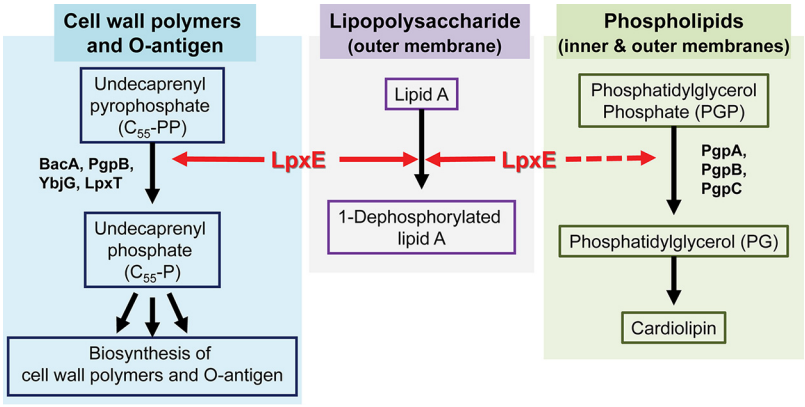

FIG 6 Multiple roles of LpxE in the biogenesis of the Gram-negative bacterial envelope. Shown is a schematic illustration of the multifunctional roles of LpxE in the biogenesis of the cell wall polymer (peptidoglycan), outer membrane (LPS), and inner membrane (PGP). Shared phosphatase activities of LpxEs from diverse bacteria, including *Aquifex* (*Aquificales*), *Francisella* (*Gammaproteobacteria*), *Rhizobium* (*Alphaproteobacteria*), and *Helicobacter* (*Epsilonproteobacteria*), toward lipid A and C_{55}-PP are indicated by solid arrows, whereas the unique PGP phosphatase activity of $LpxE_{AA}$ is indicated by a dashed red line.

can biosynthesis and the loss of O-antigen repeats in LPS associated with reduced O-antigen transport, both of which are critically dependent on the recycling of C_{55}-PP to C_{55}-P. Taken together, these results show that LpxE enzymes from *A. aeolicus* and *F. novicida* functionally connect multiple layers of bacterial envelope biogenesis and remodeling. Such multiple functional roles are not unique to LpxE enzymes from *A. aeolicus* and *F. novicida*: we found that LpxE enzymes from *H. pylori* and *R. leguminosarum* also complemented *E. coli* deficient in C_{55}-PP phosphatase activities (Fig. S6), suggesting that these LpxE enzymes can similarly process Kdo_2-lipid A and C_{55}-PP to synchronize lipid A modification with peptidoglycan biosynthesis and O-antigen modification of LPS.

It is appropriate to ask why LpxE has evolved into a multifunctional enzyme. There are several potential explanations. First, it is conceivable that the peptidoglycan biosynthesis is such an essential process that multiple enzymes, including LpxE, are employed as the backup enzymes for the C_{55}-PP phosphatase-mediated recycling reaction for peptidoglycan charging and biosynthesis. Second, it is possible that LpxE from *Aquifex* species represents an ancestral lipid phosphatase, which, although primitive, is sufficient to conduct all lipid phosphatase activities to support the bacterial envelope biogenesis and remodeling, while other LPT family of lipid phosphatases, such as the PGP phosphatase, evolved later as specialized, highly efficient enzymes. Third, it is also likely that LpxE evolved as a multifunctional enzyme to coordinate lipid A modification and the biogenesis of other layers of bacterial envelope. As 1,4′-bisphosphorylated lipid A chelates metal ions to form a fortified layer for bacterial protection, removal of the 1-phosphate could weaken the lipid A layer and increase membrane permeability. It is conceivable that the weakened lipid A layer is compensated by the elevated peptidoglycan biosynthesis and enhanced O-antigen decoration of LPS. Thus, bestowing LpxE with the multifunctionality toward Kdo_2-lipid A and C_{55}-PP (and, in the case of *A. aeolicus*, PGP) enables LpxE to orchestrate lipid A modification with bacterial envelope remodeling at multiple layers (Fig. 6) in order to promote the optimal bacterial growth and enhance bacterial survival in nature and the human host.

The Gram-negative bacterial envelope contains three layers. How Gram-negative bacteria coordinate the biogenesis and remodeling of different layers of the bacterial envelope has remained an area of active investigation. Our study has revealed the first biological evidence of a multifunctional enzyme, LpxE in *F. novicida*, that natively couples lipid A 1-dephosphorylation with C_{55}-PP recycling to enhance peptidoglycan biogenesis and O-antigen decoration of LPS, promote cell viability against antimicrobial

Downloaded from http://mbio.asm.org/ on March 4, 2020 at DUKE UNIV

peptides, evade host immune surveillance, and ultimately support bacterial pathogenesis. We suggest that such a multifunctional role represents a common but previously unappreciated mechanism for Gram-negative bacteria to coordinate bacterial envelop biogenesis across different layers.

MATERIALS AND METHODS

Data collection and refinement statistics of $LpxE_{AA}$ are listed in Table S1. All strains and plasmids used in this work are listed in Tables S2 and S3, respectively.

Plasmid and strain constructions and growth conditions are described in the supplemental material in detail.

Extraction of lipid A species, TLC and mass spectrometry analyses of lipid A species, and assay conditions are described in the Supplementary Methods section of the supplemental material.

Characterizations of *F. novicida* U112 mutants are described in the Supplementary Methods section of the supplemental material.

SUPPLEMENTAL MATERIAL

Supplemental material for this article may be found at https://doi.org/10.1128/mBio.00886-19.

TEXT S1, DOCX file, 0.1 MB.
FIG S1, TIF file, 2.8 MB.
FIG S2, TIF file, 2.8 MB.
FIG S3, TIF file, 2.9 MB.
FIG S4, TIF file, 2.8 MB.
FIG S5, TIF file, 2.8 MB.
FIG S6, TIF file, 2.2 MB.
TABLE S1, DOCX file, 0.01 MB.
TABLE S2, DOCX file, 0.02 MB.
TABLE S3, DOCX file, 0.02 MB.

ACKNOWLEDGMENTS

We thank the late professor Christian R. H. Raetz for building the foundation of this work and his mentorship.

This work was supported by the Intramural Research Program of KIST, by the Pioneer Research Center Program (2014M3C1A3054141) through the National Research Foundation of Korea funded by the Ministry of Science, ICT & Future Planning, National Research Foundation of Korea (NRF) grant founded by the Korea government (2018R1A2B2008995), and National Institutes of Health (NIH) grants (GM51310 to Christian R. H. Raetz and P.Z. and GM115355 to P.Z.). X-ray diffraction data were collected at the Northeastern Collaborative Access Team beam line 24-ID-C, which is funded by the National Institute of General Medical Sciences from the National Institutes of Health (P30 GM124165). The Pilatus 6M detector on 24-ID-C beam line is funded by a NIH-ORIP HEI grant (S10 RR029205). This research used resources of the Advanced Photon Source, a U.S. Department of Energy (DOE) Office of Science User Facility operated for the DOE Office of Science by Argonne National Laboratory under contract no. DE-AC02-06CH11357.

The funders had no role in study design, data collection and interpretation, or the decision to submit the work for publication.

REFERENCES

1. Park BS, Song DH, Kim HM, Choi BS, Lee H, Lee JO. 2009. The structural basis of lipopolysaccharide recognition by the TLR4-MD-2 complex. Nature 458:1191–1195. https://doi.org/10.1038/nature07830.
2. Shi J, Zhao Y, Wang Y, Gao W, Ding J, Li P, Hu L, Shao F. 2014. Inflammatory caspases are innate immune receptors for intracellular LPS. Nature 514:187–192. https://doi.org/10.1038/nature13683.
3. Raetz CRH, Whitfield C. 2002. Lipopolysaccharide endotoxins. Annu Rev Biochem 71:635–700. https://doi.org/10.1146/annurev.biochem.71.110601.135414.
4. Zhou P, Zhao J. 2017. Structure, inhibition, and regulation of essential lipid A enzymes. Biochim Biophys Acta Mol Cell Biol Lipids 1862:1424–1438. https://doi.org/10.1016/j.bbalip.2016.11.014.
5. Lee CJ, Liang X, Wu Q, Najeeb J, Zhao J, Gopalaswamy R, Titecat M, Sebbane F, Lemaitre N, Toone EJ, Zhou P. 2016. Drug design from the cryptic inhibitor envelope. Nat Commun 7:10638. https://doi.org/10.1038/ncomms10638.
6. Lemaitre N, Liang X, Najeeb J, Lee CJ, Titecat M, Leteurtre E, Simonet M, Toone EJ, Zhou P, Sebbane F. 2017. Curative treatment of severe Gram-negative bacterial infections by a new class of antibiotics targeting LpxC. mBio 8:e00674-17. https://doi.org/10.1128/mBio.00674-17.
7. Raetz CR, Reynolds CM, Trent MS, Bishop RE. 2007. Lipid A modification

Downloaded from http://mbio.asm.org/ on March 4, 2020 at DUKE UNIV

systems in gram-negative bacteria. Annu Rev Biochem 76:295–329. https://doi.org/10.1146/annurev.biochem.76.010307.145803.
8. Scior T, Alexander C, Zaehringer U. 2013. Reviewing and identifying amino acids of human, murine, canine and equine TLR4/MD-2 receptor complexes conferring endotoxic innate immunity activation by LPS/lipid A, or antagonistic effects by Eritoran, in contrast to species-dependent modulation by lipid IVa. Comput Struct Biotechnol J 5:e201302012. https://doi.org/10.5936/csbj.201302012.
9. Tran AX, Whittimore JD, Wyrick PB, McGrath SC, Cotter RJ, Trent MS. 2006. The lipid A 1-phosphatase of *Helicobacter pylori* is required for resistance to the antimicrobial peptide polymyxin. J Bacteriol 188:4531–4541. https://doi.org/10.1128/JB.00146-06.
10. Cullen TW, Giles DK, Wolf LN, Ecobichon C, Boneca IG, Trent MS. 2011. *Helicobacter pylori* versus the host: remodeling of the bacterial outer membrane is required for survival in the gastric mucosa. PLoS Pathog 7:e1002454. https://doi.org/10.1371/journal.ppat.1002454.
11. Carman GM. 1997. Phosphatidate phosphatases and diacylglycerol pyrophosphate phosphatases in *Saccharomyces cerevisiae* and *Escherichia coli*. Biochim Biophys Acta 1348:45–55. https://doi.org/10.1016/S0005-2760(97)00095-7.
12. Sigal YJ, McDermott MI, Morris AJ. 2005. Integral membrane lipid phosphatases/phosphotransferases: common structure and diverse functions. Biochem J 387:281–293. https://doi.org/10.1042/BJ20041771.
13. Stukey J, Carman GM. 1997. Identification of a novel phosphatase sequence motif. Protein Sci 6:469–472. https://doi.org/10.1002/pro.5560060226.
14. Dillon DA, Wu WI, Riedel B, Wissing JB, Dowhan W, Carman GM. 1996. The *Escherichia coli* pgpB gene encodes for a diacylglycerol pyrophosphate phosphatase activity. J Biol Chem 271:30548–30553. https://doi.org/10.1074/jbc.271.48.30548.
15. Wang X, Karbarz MJ, McGrath SC, Cotter RJ, Raetz CR. 2004. MsbA transporter-dependent lipid A 1-dephosphorylation on the periplasmic surface of the inner membrane: topography of *Francisella novicida* LpxE expressed in *Escherichia coli*. J Biol Chem 279:49470–49478. https://doi.org/10.1074/jbc.M409078200.
16. Karbarz MJ, Six DA, Raetz CR. 2009. Purification and characterization of the lipid A 1-phosphatase LpxE of *Rhizobium leguminosarum*. J Biol Chem 284:414–425. https://doi.org/10.1074/jbc.M808390200.
17. Plotz BM, Lindner B, Stetter KO, Holst O. 2000. Characterization of a novel lipid A containing D-galacturonic acid that replaces phosphate residues. The structure of the lipid A of the lipopolysaccharide from the hyperthermophilic bacterium *Aquifex pyrophilus*. J Biol Chem 275:11222–11228. https://doi.org/10.1074/jbc.275.15.11222.
18. Metzger LE, IV, Raetz CR. 2010. An alternative route for UDP-diacylglucosamine hydrolysis in bacterial lipid A biosynthesis. Biochemistry 49:6715–6726. https://doi.org/10.1021/bi1008744.
19. Metzger LE, Lee JK, Finer-Moore JS, Raetz CRH, Stroud RM. 2012. LpxI structures reveal how a lipid A precursor is synthesized. Nat Struct Mol Biol 19:1132–1140. https://doi.org/10.1038/nsmb.2393.
20. Altschul SF, Madden TL, Schaffer AA, Zhang J, Zhang Z, Miller W, Lipman DJ. 1997. Gapped BLAST and PSI-BLAST: a new generation of protein database search programs. Nucleic Acids Res 25:3389–3402. https://doi.org/10.1093/nar/25.17.3389.
21. Brabetz W, Muller-Loennies S, Holst O, Brade H. 1997. Deletion of the heptosyltransferase genes *rfaC* and *rfaF* in *Escherichia coli* K-12 results in an Re-type lipopolysaccharide with a high degree of 2-aminoethanol phosphate substitution. Eur J Biochem 247:716–724. https://doi.org/10.1111/j.1432-1033.1997.00716.x.
22. Yoon SH, Kim SK, Kim JF. 2010. Secretory production of recombinant proteins in *Escherichia coli*. Recent Pat Biotechnol 4:23–29. https://doi.org/10.2174/187220810790069550.
23. Fan J, Jiang D, Zhao Y, Liu J, Zhang XC. 2014. Crystal structure of lipid phosphatase *Escherichia coli* phosphatidylglycerophosphate phosphatase B. Proc Natl Acad Sci U S A 111:7636–7640. https://doi.org/10.1073/pnas.1403097111.
24. Tong SL, Lin YB, Lu S, Wang MT, Bogdanov M, Zheng L. 2016. Structural insight into substrate selection and catalysis of lipid phosphate phosphatase PgpB in the cell membrane. J Biol Chem 291:18342–18352. https://doi.org/10.1074/jbc.M116.737874.
25. Ghachi ME, Howe N, Auger R, Lambion A, Guiseppi A, Delbrassine F, Manat G, Roure S, Peslier S, Sauvage E, Vogeley L, Rengifo-Gonzalez J-C, Charlier P, Mengin-Lecreulx D, Foglino M, Touzé T, Caffrey M, Kerff F. 2017. Crystal structure and biochemical characterization of the transmembrane PAP2 type phosphatidylglycerol phosphate phosphatase from Bacillus subtilis. Cell Mol Life Sci 74:2319–2332. https://doi.org/10.1007/s00018-017-2464-6.
26. El Ghachi M, Derbise A, Bouhss A, Mengin-Lecreulx D. 2005. Identification of multiple genes encoding membrane proteins with undecaprenyl pyrophosphate phosphatase (UppP) activity in *Escherichia coli*. J Biol Chem 280:18689–18695. https://doi.org/10.1074/jbc.M412277200.
27. Lu YH, Guan Z, Zhao J, Raetz CR. 2011. Three phosphatidylglycerol-phosphate phosphatases in the inner membrane of *Escherichia coli*. J Biol Chem 286:5506–5518. https://doi.org/10.1074/jbc.M110.199265.
28. Menart V, Jevsevar S, Vilar M, Trobis A, Pavko A. 2003. Constitutive versus thermoinducible expression of heterologous proteins in Escherichia coli based on strong PR, PL promoters from phage lambda. Biotechnol Bioeng 83:181–190. https://doi.org/10.1002/bit.10660.
29. Datsenko KA, Wanner BL. 2000. One-step inactivation of chromosomal genes in Escherichia coli K-12 using PCR products. Proc Natl Acad Sci U S A 97:6640–6645. https://doi.org/10.1073/pnas.120163297.
30. Gallagher LA, Ramage E, Jacobs MA, Kaul R, Brittnacher M, Manoil C. 2007. A comprehensive transposon mutant library of *Francisella novicida*, a bioweapon surrogate. Proc Natl Acad Sci U S A 104:1009–1014. https://doi.org/10.1073/pnas.0606713104.
31. Wang X, Ribeiro AA, Guan Z, McGrath SC, Cotter RJ, Raetz CR. 2006. Structure and biosynthesis of free lipid A molecules that replace lipopolysaccharide in *Francisella tularensis* subsp. *novicida*. Biochemistry 45:14427–14440. https://doi.org/10.1021/bi061767s.
32. Kanistanon D, Hajjar AM, Pelletier MR, Gallagher LA, Kalhorn T, Shaffer SA, Goodlett DR, Rohmer L, Brittnacher MJ, Skerrett SJ, Ernst RK. 2008. A Francisella mutant in lipid A carbohydrate modification elicits protective immunity. PLoS Pathog 4:e24. https://doi.org/10.1371/journal.ppat.0040024.
33. Song F, Guan Z, Raetz CR. 2009. Biosynthesis of undecaprenyl phosphate-galactosamine and undecaprenyl phosphate-glucose in Francisella novicida. Biochemistry 48:1173–1182. https://doi.org/10.1021/bi802212t.
34. Lai XH, Shirley RL, Crosa L, Kanistanon D, Tempel R, Ernst RK, Gallagher LA, Manoil C, Heffron F. 2010. Mutations of *Francisella novicida* that alter the mechanism of its phagocytosis by murine macrophages. PLoS One 5:e11857. https://doi.org/10.1371/journal.pone.0011857.
35. Ingram BO, Sohlenkamp C, Geiger O, Raetz CR. 2010. Altered lipid A structures and polymyxin hypersensitivity of *Rhizobium etli* mutants lacking the LpxE and LpxF phosphatases. Biochim Biophys Acta 1801:593–604. https://doi.org/10.1016/j.bbalip.2010.02.001.

Downloaded from http://mbio.asm.org/ on March 4, 2020 at DUKE UNIV